CHEMISTRY OF MATERIALS

Article

pubs.acs.org/cm

Stable Artificial Solid Electrolyte Interphases for Lithium Batteries

Lin Ma,[†] Mun Sek Kim,[‡] and Lynden A. Archer*[,‡]

[†]Department of Materials Science and Engineering, Cornell University, Ithaca, New York 14853-5201, United States

[‡]School of Chemical and Biomolecular Engineering, Cornell University, Ithaca, New York 14853-5201, United States

Supporting Information

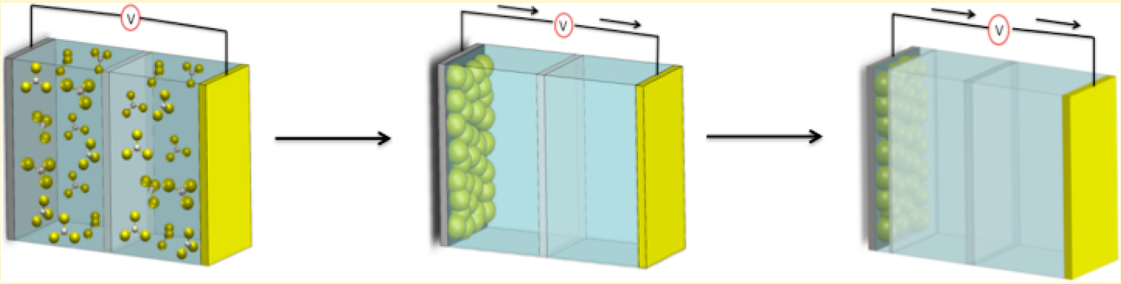

ABSTRACT: A rechargeable lithium metal battery (LMB), which uses metallic lithium as the anode, is among the most promising technologies for next generation electrochemical energy storage devices due to its high energy density, particularly when Li is paired with energetic conversion cathodes such as sulfur, oxygen/air, and oxygen−carbon dioxide mixtures. Practical LMBs in any of these designs remain elusive due to multiple problems, including parasitic reactions of Li metal with liquid electrolytes, unstable/dendritic electrodeposition at the anode during cell recharge, and chemical reaction of dissolved cathode conversion products with the Li anode. The solid electrolyte interphase (SEI) formed between lithium metal and liquid electrolytes plays a critical role in all of these processes. We report on the chemistry and interfacial properties of artificial SEI films created by in situ reaction of a strong Lewis acid AlI_3, Li metal, and aprotic liquid electrolytes. The study takes advantage of the strong surface affinity of I^- ions to initiate polymerization of dioxolane at the Li metal surface and to localize beneficial halide salts in the formed polymeric SEI thin film. We find that these SEI films impart chemical and electrochemical stability to a Li metal anode. We further show that the improvements come from at least three processes: (i) creation of a stable oligomer thin film on the Li anode, (ii) formation of a LiI salt layer at the interface, and (iii) in situ formation of a Li−Al alloy.

INTRODUCTION

Rechargeable batteries able to reliably store large amounts of electrochemical energy are needed to meet increasing demands for long-lasting, portable electrical energy storage technology for electronic devices, electric vehicles, and autonomous robotics.[1,2] Lithium-ion batteries (LIBs) are currently the technology of choice for meeting these needs; however, with current LIBs reaching the theoretical capacity limits set by the chemistry of their cathode and anode materials, a new generation of rechargeable batteries is urgently needed. The lithium metal anode has been described as the "Holy Grail" of energy storage systems due to its extremely high theoretical specific capacity (3860 mAh/g), low gravimetric density (0.59 g/cm^3), lowest negative redox potential vs standard hydrogen electrode (−3.040 V),[1,3] and the large variety of high-capacity unlithiated materials it enables as legitimate choices for the battery cathode. Thus, by replacing the carbonaceous host material used as the anode in an LIB with metallic lithium, rechargeable lithium metal batteries (LMBs) with impressive theoretical specific energies become possible.[4,5] Among these cathode materials, sulfur with a theoretical capacity of 1675 mAh/g has attracted sustained scientific interest for a variety of reasons, including its low cost, low toxicity, high natural abundance, and the fact that it undergoes spontaneous electrochemical reactions with lithium that do not require catalysts.[2,6,7]

Unfortunately, uncontrollable dendritic lithium growth and limited Coulombic efficiency during Li deposition/stripping inherent in all batteries that utilize metallic lithium as an anode have prevented broader practical applications. The formation and subsequent growth of lithium dendrites induced by inhomogeneous distribution of current density on the lithium anode may pierce the polymer separator, resulting in short circuit and subsequent thermal runaway of the cell.[3,5,8] In addition, lithium metal is reactive and over many cycles of charge and discharge will react with liquid electrolyte in contact with the metal to form fresh solid electrolyte interphases (SEIs), which ultimately consume the electrolyte, causing low cycling efficiency as the internal resistance of the cell diverges.[9,10] The already complicated chemistry at the interface of a lithium metal anode and liquid electrolyte is made even more complex when lithium metal is paired with sulfur in a lithium−sulfur (Li−S) battery, which makes these batteries an important platform for

Received: September 1, 2016
Revised: May 1, 2017
Published: May 1, 2017

DOI: 10.1021/acs.chemmater.6b03687
Chem. Mater. 2017, 29, 4181−4189

Scheme 1. Proposed Formation Mechanism for a Multifunctional Artificial Solid Electrolyte Interface (SEI) at a Li Anode Produced by AlI_3

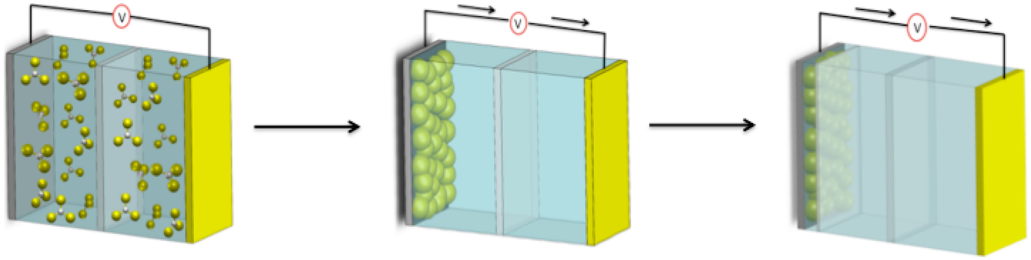

i. $3Li + AlI_3 \rightarrow 3LiI + Al$

ii. $Al + x\ Li^+ + xe^- \rightarrow Li_xAl$

iii.

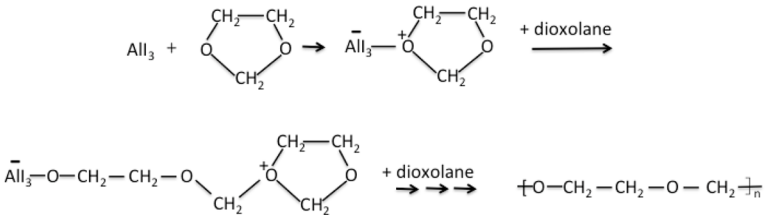

fundamental studies of how each of the degradation processes interact to cause premature failure of LMBs.

In Li−S batteries, the unique chemistry and transport behavior of soluble lithium polysulfides (LiPS) generated during discharge, lead to multiple chemical pathways in the SEI that consume Li, deplete the active anode material, and may also cause the interfacial resistance at the Li metal anode to become more inhomogeneous, which promotes rough dendritic Li deposition during cell recharge.[2,11] The products created by reduction of sulfur by lithium have been studied extensively and are now thought to include Li_2S_n species with the n value raging from 1 to 8.[2,6,12] Whereas the low order Li_2S_n ($n \leq 2$) are insoluble in most aprotic liquid electrolyte solvents, high order lithium polysulfides Li_2S_n ($n > 2$) dissolve, causing low utilization of active materials and parasitic reaction with the Li anode.[12,13] Soluble lithium polysulfides (LiPS) capable of diffusing throughout the separator also react with the Li metal anode to form insoluble and insulating sulfides on the surface of the anode, increasing the interfacial resistance and lowering both the efficiency and rate capability.[14] To solve the LiPS dissolution problem, several studies have considered novel cathode designs, including use of nanostructured carbons and metal oxides as sorbents in the cathode to provide physical trapping for LiPS,[13,15,16] specially designed additives to sequester LiPS via chemical interactions,[11,17] and polymer coatings of the cathode to provide additional transport and kinetic barriers for LiPS dissolution.[18,19] In a departure from this approach, a recent study by Ma et al.[20] showed that carbon nanotubes grafted with covalently attached polyethylenimine (PEI) chains take advantage of kinetic and thermodynamic processes to provide exceptionally high resistance to dissolution of LiPS in liquid electrolytes. Even in that case, however, the authors reported that over sufficiently long times, some amount of LiPS dissolves in the electrolyte. It means that the problem of LiPS dissolution in a Li−S cell cannot be solved through clever engineering of the cathode alone because the preferred electrolytes (e.g., dioxolane (DOL), 1,2-dimethoxyethane (DME), and tetraglyme) have high solubility for LiPS that there will always exist a chemical potential gradient between the cathode and electrolyte solvent at equilibrium, which favors dissolution and loss of LiPS to the electrolyte.

Normally, the three open problems with the Li−S cell—unstable dendritic deposition of Li at the anode during recharge; dissolution and shuttling of LiPS formed at the cathode; and uncontrolled reaction of dissolved LiPS with the anode to form resistive insoluble passivating sulfide layers—are addressed independently with novel material designs suitable for either electrode. A strategy that simultaneously sequesters sulfur in a Li−S battery cathode, protects the anode from reaction with dissolved LiPS, and at the same time eliminates dendritic deposition of Li at the nucleation step is a long sought after strategy for enabling Li−S cells able to live up to the potential of this battery technology. Herein, we report that introduction of the Lewis acid AlI_3 in DOL−DME electrolytes engenders multiple synergistic processes that enable Li−S cells with improved stability and cycling efficiency.

Our interest in AlI_3 originates from two fundamental attributes of the material: (i) The I^- ion has long been known to play a special role in adsorption phenomena in electrochemistry.[21,22] I^- belongs to the class IB adsorbents, which are known to have high surface affinity and to exhibit stronger interactions with metallic substrates than those in class IA ions or adsorbents that bond by means of simple electrostatic interactions. It is believed that these features of class 1B adsorbents originate from the donation of electrons from the adsorbing anions to available orbitals on the electrode surface. As a result, class IB anions can be adsorbed on

DOI: 10.1021/acs.chemmater.6b03687
Chem. Mater. 2017, 29, 4181−4189

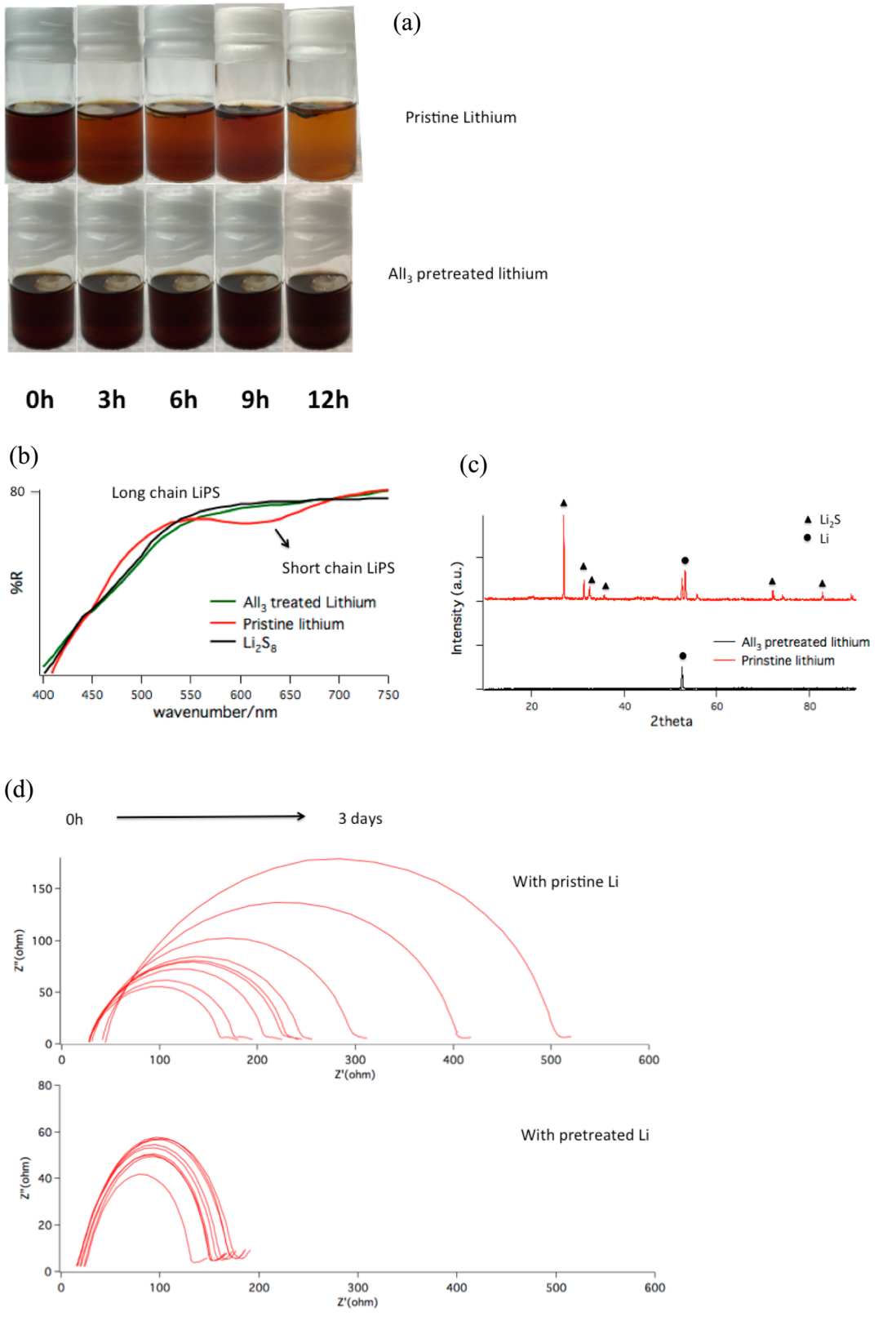

Figure 1. Chemical stability of AlI_3–DOL-treated lithium metal in a LiPS-rich electrolyte. (a) Optical images recorded at a 3 h interval of a LiPS-rich liquid electrolyte exposed to Li metal without (upper row) and with (lower row) pretreatment by AlI_3–DOL. (b) UV–vis spectra of a LiPS-rich electrolyte after exposure to lithium metal for 12 h. (c) XRD of the pristine lithium metal (red) and AlI_3–DOL-treated lithium metal foil (black) after immersion in a LiPS-rich electrolyte for 12 h. (d) Nyquist plot for a lithium symmetric cell containing a LiPS-rich electrolyte recorded in 8 h increments.

either positively charged or negatively charged surfaces with equal facility. Thus, dissociation of AlI_3 salt additives in an electrolyte in an electrochemical cell is expected to result in an I^- rich SEI layer at both electrodes. At a Li anode, it is hypothesized that the I^- bonds with Li to form a conformal LiI salt layer localized at the electrode surface. Such a LiI coating has been

DOI: 10.1021/acs.chemmater.6b03687
Chem. Mater. 2017, 29, 4181–4189

argued on the basis of recent joint density functional (JDFT) calculations to be as effective as LiF surface coatings in lowering the activation barrier for Li+ transport within the electrolyte−electrode interface,[23,24] allowing it to transport Li ions in the plane while at the same time preventing direct contact and reaction between a lithium metal anode and electrolyte solvents. (ii) AlI_3 can enhance Li cycling performance by in situ formation of a Li−Al metal alloy layer at the anode.[25] Such alloys have been reported to provide efficient barriers to Li dendrite formation, resulting in the enhancement of Li cyclability.[26−28] In the search for understanding, we also discovered that Al^{3+}, as a strong Lewis acid, is an efficient initiator for polymerization of DOL.[29] Because of the surface affinity of I^-, the polymerization reaction initiated by Al^{3+} is surface selective and produces a thin ion-conducting polymer film on the surface of lithium metal, which we believe stabilizes the lithium metal against side reactions with the electrolyte.

Scheme 1 summarizes our understanding of the specific chemical processes by which AlI_3 performs the proposed set of functions in a Li−S cell. As a proof-of concept, we first fabricated the artificial protective film on Li metal by using an electrochemical approach. The protected lithium metal was used in an additive-free (i.e., no $LiNO_3$) electrolyte to evaluate the effectiveness of the surface modification in overcoming the range of challenges with Li−S cells discussed in the Introduction. The protective SEI layer on the Li metal anode used in the demonstration was formed by cycling a symmetric lithium metal cell in a DOL/DME-1 M LiTFSI electrolyte with AlI_3 as an additive. The chemical composition of the artificial SEI and its effectiveness are presented throughout the remainder of the paper. It is understood that in a practical Li−S battery, the $LiNO_3$ additive can be reintroduced in whatever quantities desired to achieve a specific performance; here, we eliminate consideration of this additive because the goals of the study are more fundamental.

Our results show that while a wide range of conditions can be used for the pretreatment reaction, the surface reactions are self-limiting, and the beneficial attributes of the artificial SEI formed can only to a modest extent be manipulated by altering the reaction conditions. In a preferred approach, Li metal is first discharged, and then charged at constant current to a 2% depth of discharge in the electrolyte containing AlI_3. This pretreatment allows the electrochemical cleaning of lithium metal and also the complete formation of a stable SEI layer. At moderate current density (e.g., 2 mA/cm^2), the process facilitates removal of the oxide film on the lithium surface, initializing the chemical reaction between pure Li and Al^{3+}.[30] Progress of the pretreatment reactions can be followed electrochemically by measuring the voltage profile (see Supporting Information, Figure S1) and by imaging the lithium metal surface before and after treatment, as shown in Figure S2.

RESULTS AND DISCUSSION

To evaluate the effectiveness of AlI_3 as a Li surface protection agent, lithium metal foil pretreated using the approach described above was used as an electrode in both symmetric (Li/Li) and full (Li−S) cells. Lithium metal is known to react spontaneously with LiPS. Once contacted, by an electrolyte containing dissolved LiPS species, lithium metal will be oxidized by LiPS to form solid Li_2S, which will deposit onto the lithium metal surface as an undesirable insulating layer. At the same time, the reduction of the dissolved LiPS leads to a distinct color change in the electrolyte as the order *n* of the LiPS is reduced. Lithium foil with and without surface treatment was immersed in a solution of 0.05 M Li_2S_8 dissolved in tetraglyme, a good solvent for Li_2S_8, and changes in the appearance of the electrolyte and lithium metal were recorded. The results reported in the upper row of Figure 1a are for the pristine (untreated) Li foil, whereas those in the second row are typical results obtained using the AlI_3 treatment approach described above. For the pristine lithium, there is an obvious change of color of the electrolyte, indicating LiPS is reacting with lithium metal. The dark reddish color, which corresponds to high order LiPS, is observed to become markedly lighter over time. In contrast, the color of the electrolyte on the second row stays relatively dark, indicating LiPS is very stable in this case. After 12 h, the electrolyte was taken out and characterized with UV−vis spectroscopy, and the results are shown in Figure 1b. The black curve corresponds to the initial Li_2S_8 solution in tetraglyme, which shows spectra consistent with literature results for basically long chain LiPS (Li_2S_8).[31,32] In the case of pristine lithium, the UV−vis signatures for short chain LiPS are clearly evident, indicating the reduction of LiPS by reaction with lithium metal. And, consistent with the pictures shown in Figure 1a, the UV−vis spectrum of the electrolyte in contact with the pretreated Li foil is essentially identical to that of the freshly prepared electrolyte. The lithium metal immersed in the LiPS electrolyte for 12 h was removed and characterized by X-ray diffraction (XRD); results are shown in Figure 1c. It is obvious that the pristine lithium reacts with LiPS and forms Li_2S on the metal surface. However, for the pretreated lithium metal, XRD peaks for pure Li metal remain even after 12 h of exposure to LiPS, and no obvious Li_2S crystal structure is detected. Both the visualization of the color change of the electrolyte and the post-mortem analysis by UV−vis spectroscopy and XRD therefore confirm that the stability of lithium metal against LiPS is improved substantially when it is pretreated with AlI_3.

The stability of the treated Li metal in the presence of LiPS was also investigated by Electrochemical Impedance Spectroscopy (EIS) experiments. Symmetric Li/Li cells using either pristine Li (control) or AlI_3 treated Li were employed in these experiments, and the electrolyte is deliberately reinforced with 0.1 M Li_2S_8 (Figure 1d). The impedance is characterized as a function of time, which provides an indication of the lithium corrosion level by reacting with LiPS in the electrolyte. Both the real (resistance) and imaginary (capacitance) parts of the impedance are seen to increase more for the control cells. In particular the real part of the impedance of the control cells is seen to increase rapidly, reaching a value of around 250% of the initial value after 72 h. In contrast, cells containing protected lithium are noticeably less reactive when in contact with a LiPS-rich electrolyte—only a 45% increase is observed for the impedance over 72 h. Following these measurements, the Li electrodes were harvested and the surface morphology of lithium metal observed using scanning electron microscopy (SEM). For the unprotected lithium metal, the lithium surface is seen to be very rough, indicating the severe erosion of lithium metal by LiPS; however, the pretreated lithium has much less roughness (Figure S3).

A remarkable and synergetic benefit of the AlI_3 surface treatment revealed by the proposed reaction mechanism in Scheme 1 is that both the LiI layer and Li−Al alloys formed at the interface should stabilize Li metal against dendrite formation during cell cycling. To investigate these effects, symmetric (Li/Li) cells containing pristine and AlI_3-treated Li foil were assembled. A standard polypropylene membrane (Celgard) was used as the separator and 1 M LiTFSI in DOL/DME (v/v = 1:1) was applied as the electrolyte. To evaluate the stability of the

DOI: 10.1021/acs.chemmater.6b03687
Chem. Mater. 2017, 29, 4181−4189

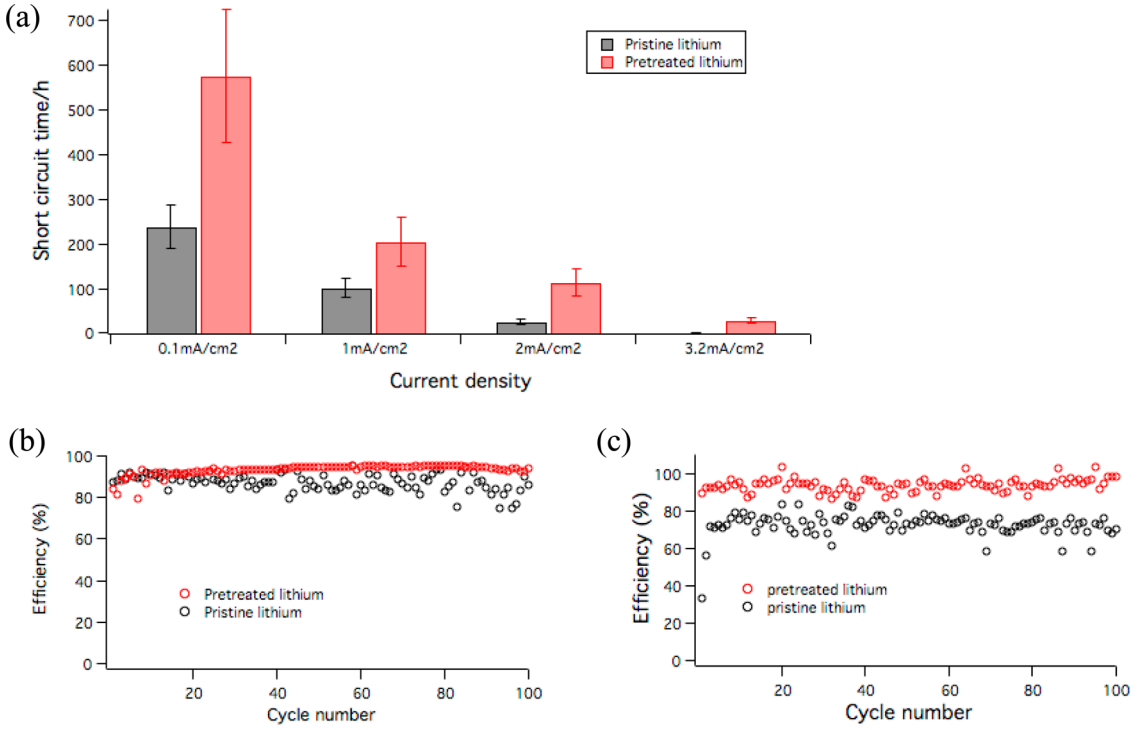

Figure 2. Lithium dendrite resistance and Coulombic efficiency of AlI_3–DOL-treated lithium metal. (a) Short circuit time for symmetric Li/Li cells deduced from galvanostatic polarization measurements at different current densities. The dark gray column represents the control case in which pristine lithium is used; the light gray column shows the short circuit time for cells based on AlI_3–DOL-treated lithium metal. (b and c) Lithium deposition efficiency in Li/electrolyte/stainless steel cells comprised of pristine lithium and AlI_3–DOL-treated lithium metal electrodes, respectively. In these experiments, the cell is discharged for 30 min at a constant current density and then recharged to 0.5 V at the same current density. (b) Current density = 0.2 mA/cm^2. (c) Current density = 2 mA/cm^2.

cells to failure by dendrite-induced short circuiting, galvanostatic polarization measurements were performed in which lithium is continuously stripped from one electrode and plated on the other at a fixed current density; cell failure in this experiment occurs when the measured voltage is observed to drop discontinuously (see Supporting Figure S4) as the internal short lowers the cell resistance.[33] Figure 2a reports the cell lifetimes at various current densities. It is seen that the lifetime or short-circuit time t_c is greatly improved when lithium metal is protected with an SEI layer involving AlI_3. The improvement is more obvious when a higher current is applied and the resultant t_{sc} values at 3 mA/cm^2 are the highest reported in the literature for this experiment.[3,33] It should also be noted that the electrolyte used in these experiments contains no additives, which means that the SEI layer is quite stable by itself over lithiation over a long period.

The Coulombic efficiency (CE) provides a simple measure of the effectiveness of the Li surface protection offered by the AlI_3 treatment. CE was examined using a Li/electrolyte/stainless steel cell design, which allows the lithium loss on cycling to be accurately determined as the amount of lithium stripped divided by the amount of lithium plated on the stainless steel foil. A fixed amount of lithium is stripped from the lithium metal at a constant discharge current and deposited onto stainless steel, followed by a charge process where all the lithium is transported back to the lithium electrode.[34] Figure 2b and c show the Coulombic efficiency versus cycle number for cells with 1 M LiTFSI in DOL/DME (v/v = 1:1) at current densities of 0.2 mA/cm^2 and 2 mA/cm^2 (Figure 2b and c, respectively). The black curve is the control case, in which pristine lithium is used, and the red curve represents the pretreated lithium. In Figure 2b, when pretreated lithium metal is used, the CE is stable at ~95%, while there is fluctuation in the cell with pristine lithium. There is nonetheless still loss of efficiency with the protection of AlI_3, which might be due to the exposed lithium on stainless steel reacting with the electrolyte. The improvement is still observed when the current density is increased to 2 mA/cm^2 (Figure 2c), where the efficiency is increased from ~70% to ~92% when lithium metal is pretreated with AlI_3. Figure S5 reports the CE for electrolytes in which LiPS is directly added to promote parasitic reactions with the freshly deposited Li metal. The addition of LiPS to the electrolyte is observed to dramatically decrease the stability of the control cell, resulting in large fluctuations in efficiency when pristine lithium is used. However, consistent with what we found in Figure 1, the pretreated lithium metal shows improved stability against LiPS, and the cycling is much more stable with an improved efficiency to ~91% over 100 cycles.

The results reported in Figures 1 and 2 therefore demonstrate the effectiveness of AlI_3 as an additive in the formation of a stable SEI layer on Li metal. The results also show that treatment of Li metal with AlI_3 improves its stability against corrosion by LiPS, enhances its resistance to failure by lithium dendrite formation, and improves the Coulombic efficiency of the cell. Before illustrating the benefits of these effects in a Li–S cell, we consider how AlI_3 performs these functions in detail.

Figure S6 shows the impedance for symmetric cells before and after treatment with AlI_3. The solid lines correspond to the cells before cycling. The cells containing AlI_3 in the electrolyte already show lower impedance compared with the control case. We infer that there may already be a SEI layer formed before electrochemical treatment so that the conductive LiI layer leads to lower impedance. After a single cycle, the impedance of

DOI: 10.1021/acs.chemmater.6b03687
Chem. Mater. 2017, 29, 4181−4189

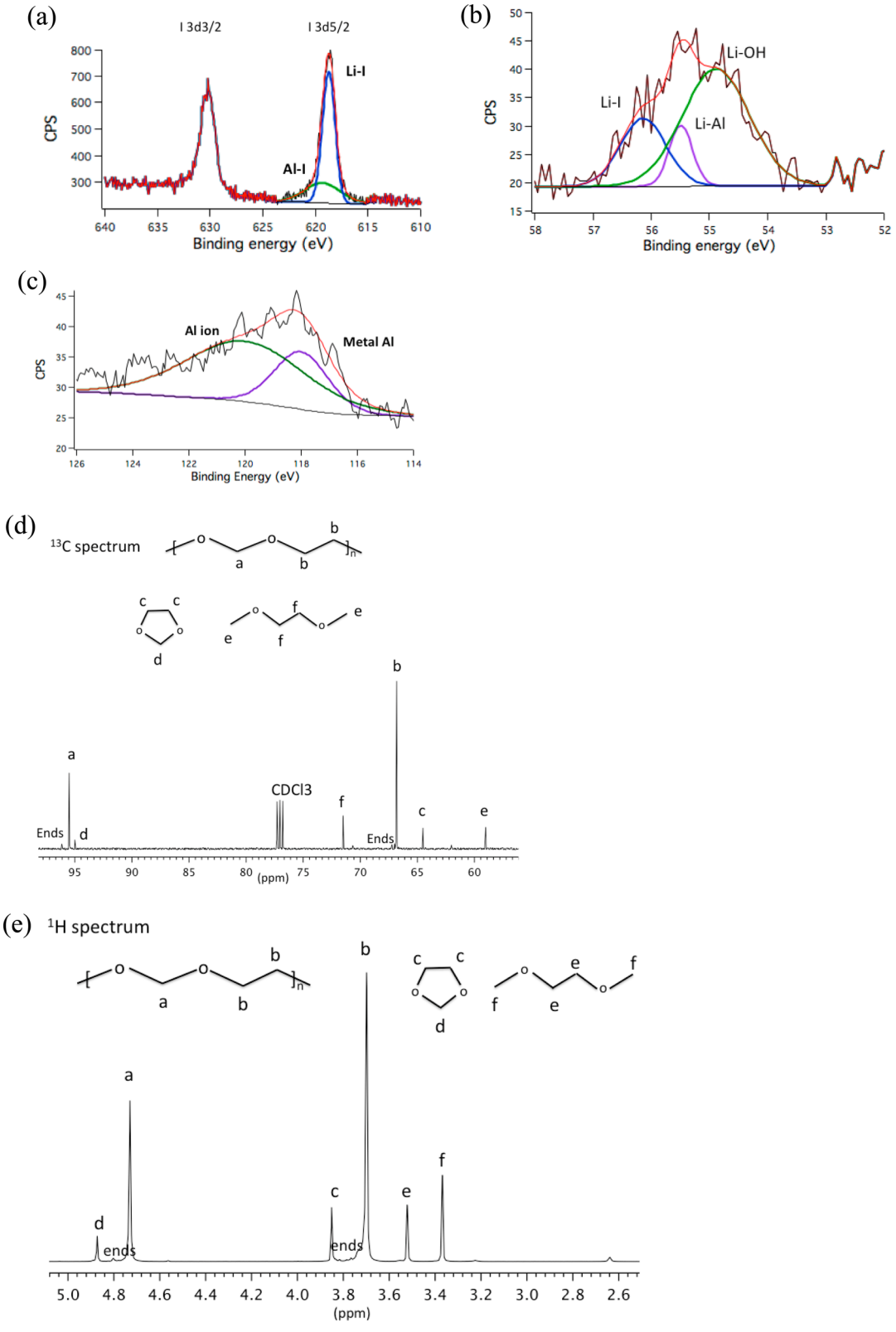

Figure 3. Characterization of the AlI_3–DOL-treated lithium metal by XPS and NMR. (a, b and c) High resolution XPS spectra for AlI_3–DOL-treated lithium metal. (a) I 3d spectra; (b) Li 1s spectra; (c) Al 2s spectra. (d and e) NMR of the polymeric gel. (d) ^{13}C NMR spectrum. (e) ^{1}H NMR spectrum.

AlI_3 is observed to shrink substantially. This may be due to formation of a more complete SEI layer after the cleaning of the lithium surface and the strong adsorption of the I^- anion on the electrodes. In contrast, for the control case, the impedance does not change too much before and after the treatment. It might be because after cleaning the lithium surface, it immediately reacts with the electrolyte solvents and again forms lithium oxidation products, such as lithium hydroxide or other lithium oxides, which has similar interfacial chemistry and transport properties with the pristine surface and results in similar impedance.

DOI: 10.1021/acs.chemmater.6b03687
Chem. Mater. 2017, 29, 4181−4189

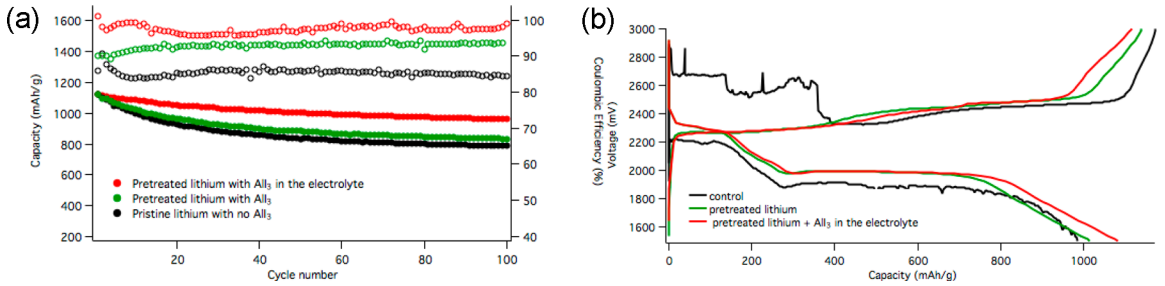

Figure 4. Electrochemical measurements employing Li−S cells containing AlI_3−DOL-treated lithium metal as an anode and at a current rate of 0.5C. These cells do not contain $LiNO_3$ electrolyte additives typically used in Li−S battery studies. (a) Comparison of cycling performance of Li−S cells based on AlI_3−DOL-treated and untreated Li metal anodes. The black filled symbols denote the specific capacity of cells based on pristine lithium metal anodes with additive free electrolyte. The green filled symbols are specific capacities of cells based on AlI_3−DOL-treated Li anodes with additive-free electrolyte. The red filled symbols denote specific capacities of cells based on AlI_3−DOL-treated Li anodes and DOL/DME-based electrolytes containing AlI_3 as an additive. The open symbols are the respective Coulombic efficiency. (b) The corresponding voltage profiles for Li−S cells in each of the configurations reported in part a.

The pretreated lithium metal was harvested and washed thoroughly with DOL/DME and its surface chemistry characterized by means of XPS. Figure 3a shows a strong I 3d signal, which has well separated spin−orbit components with an energy separation of 11.5 eV. The deconvolution of I 3d 5/2 shows both Li−I and Al−I peaks, which is consistent with our hypothesis of strong I^- ion adsorption. Also, the Li 1s peak (Figure 3b) can be deconvoluted into Li−I (56.1 eV), Li−Al alloy (55.5 eV), and Li−OH (54.9 eV) peaks, which is consistent with the NIST database and literature reports.[35,36] We suspect that the hydroxides may be formed during the sample transfer or the reaction between lithium and the solvents. Again, this is consistent with our hypothesis that there is formation of Li−I and Li−Al alloy during the discharge and charge process, which can help to stabilize lithium metal. Al signals are also detected in the XPS spectra. Deconvolution of the Al 2s peak (Figure 3c) shows both the metal Al (120 eV)[29] and Al ion (∼118 eV) peaks,[37] confirming the existence of Al metal and Al ions on the surface, providing a clue for Li/Al alloy formation and Al^{3+} adsorption on the electrode surface.

Following galvanostatic polarization, post-mortem characterization of the lithium metal electrode was carried out using XPS and SEM analysis. It is significant that the signatures of Al and I are still apparent from the XPS spectra (Figure S7b and c) of the pretreated material after polarization. It indicates that the SEI layer formed by the reaction of Li and AlI_3 is stable even after cells are short-circuited in a polarization experiment. What's perhaps even more interesting is that, even after the cell shorts, the film-like appearance of the Li metal coating remains largely intact (Figure S8a). The film structure seems to be punctured through by the lithium dendrite growth. The film was also observed to form spontaneously as an upper (lower-density phase) in an AlI_3 containing electrolyte (Figure S8b) after the electrolyte was rested for a period of about 2 weeks in an Ar-filled glovebox. The gel-like membrane was separated from the liquid electrolyte and washed with DOL/DME to get rid of any interred salts and was characterized by gel permeation chromatography (GPC). Analysis of the results reported in Figure S9a using polystyrene standards shows that the material is a polymer with a number-averaged molecular weight $M_n \approx 2200$ g/mol, weight-averaged molecular weight $M_w \approx 3380$ g/mol, and polydispersity index PDI = $M_w/M_n = 1.5$.

In order to investigate the chemistry and structure of the polymer, mass spectra and NMR measurements were performed. Figure S9b shows that a series of species/fragments with a mass difference of 74 is observed. This mass increment is exactly the molecular weight of DOL, meaning that the film formed in the AlI_3-containing electrolytes is polyDOL. NMR analysis (Figure 3d and e) confirms that the gel is composed of polymerized DOL with a structure of *n*-[−O−CH_2−O−CH_2−CH_2−]−*n*. Both the ^{13}C and ^1H spectra match pretty well with the proposed structure. They also show peaks for DOL and DME small molecules due to the solvent residue in the gel, which disappear when the gel is tested with diffusion ordered ^1H NMR (Figure S10), where the polymer signals remain as slow diffusers. Thus, the information provided by GPC, mass spectra, and NMR spectra reveal that the gel is the product of DOL polymerization. Our finding, while important, is not surprising since the ring opening of DOL is already known to be initiated by Lewis acid acting as an initiator and was one of the reasons we chose to work with AlI_3 as a strong Lewis acid able to attack the nucleophile center on the O atom and initiate the polymerization of DOL,[38−40] and the detailed reaction mechanism could be found in some related polymer chemistry studies.[41,42]

Figure 4 reports the electrochemical characteristics of Li−S cells based on the AlI_3-treated Li metal anodes at a current rate of 0.5C. The cathode used in these experiments was prepared by the methods reported earlier, where sulfur is infused into amine-functionalized CNT.[20] The green plot in Figure 4a corresponds to the control case, where pristine lithium metal is used, and the black curve represents pretreated lithium metal being used as an anode. The capacity is very similar between the two cases, while the efficiency is increased from 83% to 92%. Extra capacity is observed in the pretreated case because the reaction between LiPS and lithium metal is mitigated and more LiPS is available to contribute to the capacity. What is more interesting is that, when additional AlI_3 is introduced to the electrolyte, both the capacity and efficiency rise, with the CE exceeding 97% by the 100th cycle. We suspect that this benefit of utilizing additional AlI_3 in the Li−S electrolyte stems from the ability of AlI_3 to repair any defects in the surface coating formed during the pretreatment or by reaction with LiPS in the cycled electrolyte. The need for such repair is evident in Figure 1d, where the impedance of the symmetric cell using AlI_3-treated lithium also increases to some extent, suggesting the formation of a certain amount of Li_2S on the lithium surface. This observation also implies that interactions between the AlI_3 electrolyte additive and components in the cathode of an electrochemical full cell can be nontrivial and require careful investigation.

DOI: 10.1021/acs.chemmater.6b03687
Chem. Mater. 2017, 29, 4181−4189

The voltage profile in Figure 4b shows that during cycling the overpotential in both the discharge and charge process is greatly suppressed when AlI_3 is incorporated. Figure S11 shows the cyclic voltammetry of the Li−S battery applying the pretreated lithium as the anode. The peaks show typical characteristics of sulfur reduction and oxidization, and the stable position of the peaks indicates stable electrochemical reaction of sulfur.

In conclusion, an electrochemical strategy in which AlI_3 is used to initiate polymerization of a DOL/DME-based electrolyte to form a stable artificial SEI coating to protect the lithium metal anode is presented. The procedure leads to the formation of a surface coating on Li that includes LiI, Li−Al, and a thin polymer film. The polymer film is shown by means of mass spectrometry, gel permeation chromatography, and NMR to be an oligomer with a weight-average molecular weight of 3380 g/mol that results from polymerization of DOL initiated by Al^{3+}. When the pretreated lithium metal is used as the electrode in symmetric Li/Li cells or as an anode in Li−S cells, the stability of the electrode is shown to be greatly improved by multiple synergistic processes. These processes include the effect of LiI and Li−Al in stabilizing electrodeposition of Li against dendrite formation and protection of the Li anode in the Li−S cell from reaction with soluble LiPS, therefore reducing shuttling and anode surface passivation. The promising electrochemical results and scientific understanding made possible by the study underscore the promise of AlI_3 and other strong Lewis acids as initiators for the formation of stable, self-limited polymer films that provide artificial SEI coatings to stabilize performance of electrochemical cells based on high-capacity conversion cathodes and metallic anodes.

MATERIALS AND METHODS

Pretreatment of Lithium Metal with AlI_3. A symmetric cell (Li/electrolyte/Li) was assembled and used to create tethered polymer coatings on Li. A total of 40 μL of 1 M LiTFSI and 600 ppm of AlI_3 dissolved in DOL/DME (v/v = 1:1) was used as an electrolyte. The electrolyte solvents were dried over 3 Å molecular sieves; the salts were dried at 100 °C under a vacuum. All electrolyte components were stored in an argon-filled glovebox prior to use, and the electrolyte was prepared by mixing these components with a Teflon-coated stir bar in the glovebox. The moisture content of electrolytes produced in this manner was quantified by Karl Fischer titration (Mettler Toledo C20 KF titrator) and found to be <20 ppm. The symmetric cell was discharged at a current density of 2 mA/cm^2, at a depth of 2% DOD, followed by a charge process at the same current density. The cell was opened in an Ar-filled glovebox and the anode retrieved for surface characterization and electrochemical analysis. Whereas coated anode samples for electrochemical analysis were directly transferred to sealed electrochemical cells in the same Ar-filled glovebox, those used for our surface characterization experiments had to be removed from the glovebox.

Preparation of Li_2S_8 for LiPS stability study. Li_2S_8 was prepared following Rauh[43] et al.'s procedure in a solution process where stoichiometric amounts of elemental sulfur and Li_2S were codissolved into tetraglyme, followed by heating at 80 °C with stirring for 6 h.

Characterization. The LiPS species in the electrolyte were analyzed using a Shimadzu UV−vis spectrometer. The crystalline structure was characterized using a Scintag Theta−Theta X-ray Diffractometer (XRD). Morphologies of the electrodes were studied using LEO 1550 FESEM (Keck SEM) and FEI Tecnai G2 T12 Spirit TEM (120 kV). Impedance spectra were recorded as a function of frequency using a Novocontrol N40 broadband dielectric spectrometer. X-ray photoelectron spectroscopy (XPS) was used for elemental analysis and to obtain chemical information on films formed on the Li electrode. Gel permeation chromatography (GPC) was utilized to characterize the molecular weight of the polymer coating on the lithium anode. The polymer was dissolved in tetrahydrofuran (THF) to form a solution with a concentration 1 mg/mL, and a Waters Ambient-Temperature GPC operated at 40 °C with an elution rate of 1.0 mL/min was employed to recover the elutogram for the solution. Polystyrene standards with molecular weight in the range 10^3 D to 10^6 D (PSS USA; Amherst, MA) were used as a reference to estimate the molecular weight of the polymer from the elutogram. The polymer composition was investigated using a JEOL AccuTOF-DART (Direct Analysis in Real Time) ambient ionization mass spectrometer, and its structure was analyzed using an INOVA 400 NMR facility.

Electrochemical Characterization. The sulfur cathode composite CNT-PEI/S is prepared as described in a previous study,[20] and the sulfur content in the composite is 60%. 2030 coin-type cells were assembled using lithium metal (0.76-mm-thick, Alfa Aesar) as the anode electrode, a microporous material, Celgard 2500, membranes as separators, a cathode with 80% as prepared CNT-PEI/S composite, 10% Super-P Li carbon black from TIMCAL, and 10% poly(vinylidene difluoride) (PVDF, Sigma-Aldrich) as a binder in an excess of *N*-methyl-2-pyrrolidone in NMP, and an electrolyte of 40 μL of 1 M lithium bis(trifluoromethanesulfone) imide (LiTFSI) for each cell. The sulfur loading per electrode is 1.2 mg/cm^2. Cell assembly was carried out in an argon-filled glovebox (MBraun Labmaster). The room-temperature cycling characteristics of the cells were evaluated under galcanostatic conditions using Neware CT-3008 battery testers and electrochemical processes in the cells were studied by cyclic voltammetry using a CHI600D potentiostat.

ASSOCIATED CONTENT

Supporting Information

The Supporting Information is available free of charge on the ACS Publications website at DOI: 10.1021/acs.chemmater.6b03687.

Additional electrochemical testing results and supplemental mass spectra, XPS, SEM, GPC, and NMR data (PDF)

AUTHOR INFORMATION

Corresponding Author

*E-mail: laa25@cornell.edu.

ORCID

Lynden A. Archer: 0000-0001-9032-2772

Notes

The authors declare the following competing financial interest(s): Professor Archer is a founder of NOHMs Technologies, a technology concern focused on commercializing electrolytes and electrode materials for lithium ion and lithium-sulfur batteries.

ACKNOWLEDGMENTS

The authors acknowledge support from the National Science Foundation Division of Materials Research Award No. DMR 1609125. Electron microscopy, X-ray diffraction, X-ray photoelectron spectroscopy facilities, and optical spectrometers available through the Cornell Center for Materials Research (CCMR) were used for this work (NSF Grant DMR-1120296).

REFERENCES

(1) Tarascon, J. M.; Armand, M. Issues and challenges facing rechargeable lithium batteries. *Nature* **2001**, *414*, 359−367.

(2) Ma, L.; Hendrickson, K. E.; Wei, S.; Archer, L. A. Nanomaterials: Science and applications in the lithium−sulfur battery. *Nano Today* **2015**, *10*, 315−338.

(3) Lu, Y.; Tu, Z.; Archer, L. A. Stable lithium electrodeposition in liquid and nanoporous solid electrolytes. *Nat. Mater.* **2014**, *13*, 961−969.

DOI: 10.1021/acs.chemmater.6b03687
Chem. Mater. 2017, 29, 4181−4189

(4) Lu, Y.; Tikekar, M.; Mohanty, R.; Hendrickson, K.; Ma, L.; Archer, L. A. Stable cycling of lithium metal batteries using high transference number electrolytes. *Adv. Energy Mater.* **2015**, *5*, 1402073.
(5) Armand, M.; Tarascon, J. M. Building better batteries. *Nature* **2008**, *451*, 652−657.
(6) Guo, J.; Yang, Z.; Yu, Y.; Abruna, H. D.; Archer, L. A. Lithium-sulfur battery cathode enabled by lithium-nitrile interaction. *J. Am. Chem. Soc.* **2013**, *135*, 763−767.
(7) Cohn, G.; Ma, L.; Archer, L. A. A novel non-aqueous aluminum sulfur battery. *J. Power Sources* **2015**, *283*, 416−422.
(8) Tikekar, M. D.; Choudhury, S.; Tu, Z.; Archer, L. A. Design principles for electrolytes and interfaces for stable lithium-metal batteries. *Nature Energy* **2016**, *1*, 16114.
(9) Chazalviel, J. N. Electrochemical aspects of the generation of ramified metallic electrodeposits. *Phys. Rev. A: At., Mol., Opt. Phys.* **1990**, *42*, 7355−7367.
(10) Bouchet, R.; Maria, S.; Meziane, R.; Aboulaich, A.; Lienafa, L.; Bonnet, J.-P.; Phan, T. N. T.; Bertin, D.; Gigmes, D.; Devaux, D.; Denoyel, R.; Armand, M. Single-ion BAB triblock copolymers as highly efficient electrolytes for lithium-metal batteries. *Nat. Mater.* **2013**, *12*, 452−457.
(11) Ma, L.; Zhuang, H.; Lu, Y.; Moganty, S. S.; Hennig, R. G.; Archer, L. A. Tethered molecular sorbents: enabling metal-sulfur battery cathodes. *Adv. Energy Mater.* **2014**, *4*, 1400390.
(12) Manthiram, A.; Fu, Y.; Chung, S.-H.; Zu, C.; Su, Y.-S. Rechargeable lithium−sulfur batteries. *Chem. Rev.* **2014**, *114*, 11751−11787.
(13) Jayaprakash, N.; Shen, J.; Moganty, S. S.; Corona, A.; Archer, L. A. Porous hollow Carbon@Sulfur composites for high-power lithium−sulfur batteries. *Angew. Chem., Int. Ed.* **2011**, *50*, 5904−5908.
(14) Hendrickson, K. E.; Ma, L.; Cohn, G.; Lu, Y.; Archer, L. A. Model membrane-free Li−S batteries for enhanced performance and cycle fife. *Adv. Sci.* **2015**, *2*, 1500068.
(15) Wang, H.; Yang, Y.; Liang, Y.; Robinson, J. T.; Li, Y.; Jackson, A.; Cui, Y.; Dai, H. Graphene-wrapped sulfur particles as a rechargeable lithium−sulfur battery cathode material with high capacity and cycling stability. *Nano Lett.* **2011**, *11*, 2644−2647.
(16) Ji, X.; Lee, K. T.; Nazar, L. F. A highly ordered nanostructured carbon-sulphur cathode for lithium-sulphur batteries. *Nat. Mater.* **2009**, *8*, 500−506.
(17) Ma, L.; Wei, S.; Zhuang, H. L.; Hendrickson, K. E.; Hennig, R. G.; Archer, L. A. Hybrid cathode architectures for lithium batteries based on TiS2 and sulfur. *J. Mater. Chem. A* **2015**, *3*, 19857−19866.
(18) Zheng, G.; Zhang, Q.; Cha, J. J.; Yang, Y.; Li, W.; Seh, Z. W.; Cui, Y. Amphiphilic surface modification of hollow carbon nanofibers for improved cycle life of lithium sulfur batteries. *Nano Lett.* **2013**, *13*, 1265−1270.
(19) Zhou, W.; Chen, H.; Yu, Y.; Wang, D.; Cui, Z.; DiSalvo, F. J.; Abruña, H. D. Amylopectin wrapped graphene oxide/sulfur for improved cyclability of lithium−sulfur battery. *ACS Nano* **2013**, *7*, 8801−8808.
(20) Ma, L.; Zhuang, H.; Wei, S.; Hendrickson, K. E.; Kim, M. S.; Cohn, G.; Hennig, R. G.; Archer, L. A. Enhanced Li-S batteries using amine-functionalized carbon nanotubes in the cathode. *ACS Nano* **2016**, *10*, 1050−1059.
(21) Anson, F. C. Patterns of ionic and molecular adsorption at electrodes. *Acc. Chem. Res.* **1975**, *8*, 400−407.
(22) Ishikawa, M.; Kawasaki, H.; Yoshimoto, N.; Morita, M. Pretreatment of Li metal anode with electrolyte additive for enhancing Li cycleability. *J. Power Sources* **2005**, *146*, 199−203.
(23) Gunceler, D.; Schwarz, K.; Sundararaman, R.; Letchworth-Weaver, K.; Arias, T. In *16th International Workshop on Computation Physics and Materials Science: Total Energy and Force Methods*; International Centre for Theoretical Physics: Trieste, Italy, 2012.
(24) Gunceler, D.; Letchworth-Weaver, K.; Sundararaman, R.; Schwarz, K. A.; Arias, T. A. The importance of nonlinear fluid response in joint density-functional theory studies of battery systems. *Modell. Simul. Mater. Sci. Eng.* **2013**, *21*, 074005−074022.
(25) Dey, A. N. Electrochemical alloying of lithium in organic electrolytes. *J. Electrochem. Soc.* **1971**, *118*, 1547−1549.
(26) Fauteux, D.; Koksbang, R. Rechargeable lithium battery anodes-alternatives to metallic lithium. *J. Appl. Electrochem.* **1993**, *23*, 1−10.
(27) Baranski, A. S.; Fawcett, W. R. The formation of lithium-aluminum alloys at an aluminum electrode in propylene carbonate. *J. Electrochem. Soc.* **1982**, *129*, 901−907.
(28) Zlatilova, P.; Balkanov, I.; Geronov, Y. Thin foil lithium-aluminium electrode. The effect of thermal treatment on its electrochemical behaviour in nonaqueous media. *J. Power Sources* **1988**, *24*, 71−79.
(29) Dohmeier, C.; Loos, D.; Schnockel, H. Aluminum (I) and Gallium (I) Compounds: synthesis, structures, and reactions. *Angew. Chem., Int. Ed. Engl.* **1996**, *35*, 129−149.
(30) Aurbach, D.; Weissman, I.; Yamin, H.; Elster, E. The correlation between charge:discharge rates and morphology, surface chemistry, and performance of Li electrodes and the connection to cycle life of practical batteries. *J. Electrochem. Soc.* **1998**, *145*, 1421−1426.
(31) Patel, M. U.; Demir-Cakan, R.; Morcrette, M.; Tarascon, J. M.; Gaberscek, M.; Dominko, R. Li-S battery analyzed by UV/Vis in operando mode. *ChemSusChem* **2013**, *6*, 1177−1181.
(32) Xu, W. T.; Peng, H. J.; Huang, J. Q.; Zhao, C. Z.; Cheng, X. B.; Zhang, Q. Towards stable lithium-sulfur batteries with a low self-discharge rate: ion diffusion modulation and anode protection. *ChemSusChem* **2015**, *8*, 2892−2901.
(33) Khurana, R.; Schaefer, J. L.; Archer, L. A.; Coates, G. W. Suppression of lithium dendrite growth using cross-linked polyethylene/poly(ethylene oxide) electrolytes: a new approach for practical lithium-metal polymer batteries. *J. Am. Chem. Soc.* **2014**, *136*, 7395−7402.
(34) Li, W.; Yao, H.; Yan, K.; Zheng, G.; Liang, Z.; Chiang, Y.-M.; Cui, Y. The synergetic effect of lithium polysulfide and lithium nitrate to prevent lithium dendrite growth. *Nat. Commun.* **2015**, *6*, 7436.
(35) NIST X-ray Photoelectron Spectroscopy Database. https://srdata.nist.gov/xps/default.aspx.
(36) Xie, K.; Duan, L.; Zhang, D.; Qiao, J.; Dong, G.; Wang, L.; Qiu, Y. Formation, confirmation and application of Li: Al alloy as an electron injection layer with Li3N as the precursor. *J. Phys. D: Appl. Phys.* **2010**, *43*, 252001−252004.
(37) Feliu, S., Jr.; Samaniego, A.; Bermudez, E.; El-Hadad, A.; Llorente, I.; Galván, J. Effect of native oxide film on commercial magnesium alloys substrates and carbonate conversion coating growth and corrosion resistance. *Materials* **2014**, *7*, 2534−2560.
(38) Aurbach, D. Review of selected electrode−solution interactions which determine the performance of Li and Li ion batteries. *J. Power Sources* **2000**, *89*, 206−218.
(39) Gofer, Y.; Einely, Y.; Aurbach, D. Surface chemistry of lithium in 1,3-dioxolane. *Electrochim. Acta* **1992**, *37*, 1897−1899.
(40) Aurbach, D.; Youngman, O.; Gofer, Y.; Meitav, A. The electrochemical behaviour of 1,3-dioxolane—LiClO4 solutions—I. Uncontaminated solutions. *Electrochim. Acta* **1990**, *35*, 625−638.
(41) Okada, M.; Yamashita, Y.; Ishii, Y. Polymerization of 1,3-Dioxolane. *Makromol. Chem.* **1964**, *80*, 196−207.
(42) Sasaki, S.; Takahashi, Y.; Tadokoro, H. Structural studies of polyformals, [−OCH2O−(CH2)m−]n. I. poly (1,3-dioxepane). *Polym. J.* **1973**, *4*, 172−182.
(43) Rauh, R. D.; Abraham, K. M.; Pearson, G. F.; Surprenant, J. K.; Brummer, S. B. A Lithium/dissolved sulfur battery with an organic electrolyte. *J. Electrochem. Soc.* **1979**, *126*, 523−527.

DOI: 10.1021/acs.chemmater.6b03687
Chem. Mater. 2017, 29, 4181−4189